SURFACE and INTERFACE ANALYSIS

Received: 31 October 2013 Revised: 24 January 2014 Accepted: 29 January 2014 Published online in Wiley Online Library: 21 March 2014

(wileyonlinelibrary.com) DOI 10.1002/sia.5423

How material properties affect depth profiles – insight from computer modeling

Robert J. Paruch,[a]* Zbigniew Postawa[b] and Barbara J. Garrison[a]

A previously developed steady-state statistical sputtering model (SS-SSM) is useful for interpretation of molecular dynamics (MD) simulations of repetitive bombardment. This method is applicable to computer modeling of depth profiling. In this paper, we demonstrate how the formalism provided by SS-SSM is used to identify the factors that determine the depth resolution of δ-layer depth profiling. The analysis is based on MD simulations of repetitive keV C_{60} bombardment of coinage metal samples. The results show that the primary dependence of the depth profiling quality is on the sample binding energy, with bigger binding energies giving better depth resolution. The effects of sample atom mass and surface opacity are also discussed. Copyright © 2014 John Wiley & Sons, Ltd.

Keywords: cluster sputtering; depth profiling; molecular dynamics; sputtering model; computer modeling

Introduction

Molecular depth profiling with SIMS became tractable when cluster ion beam sources were introduced.[1] Concurrently, molecular dynamics (MD) simulations were employed as the theoretical partner to the SIMS technique in order to explain the factors for depth profiling.[2,3] A 'divide and conquer' MD protocol for repetitive bombardment was proposed to model dynamic SIMS experiments.[4] Although it was possible to calculate directly from MD results certain quantities that limit the depth resolution of depth profiling, such as root mean square (RMS) roughness and sputtering yields, obtaining the depth profiles remained beyond the MD simulation capabilities.[5,6] These massive calculations in several months of computing time were able to remove only a few nanometers of material from the sample, which was much less than is typically removed during depth profiling experiments. Because the MD simulation of repetitive bombardment contains all the information that is needed to calculate an appropriate depth profile, including properties of sample material, incident cluster type, and primary beam conditions, the issue was how to utilize the results based on limited scale MD simulations to predict depth profiles.

In order to deal with this issue, we developed an analytic model to extrapolate the simulation results toward fluence ranges corresponding to removal of tens to hundreds of nanometers of material. The steady-state statistical sputtering model (SS-SSM) utilizes the information from the steady-state of the 'divide and conquer' MD simulation and gives the depth profile of a δ-layer buried in the sample.[7] This model is a revised form of the statistical sputtering model previously developed by Krantzman and Wucher.[8] Although the input MD simulations still take months of computer time, the SS-SSM allows us to calculate depth profiles in a couple of hours of computing time.

The SS-SSM provides a framework for describing processes that take place during simulations of repetitive bombardment as is appropriate for depth profiling. Consequently, the factors that influence the quality of depth profiling can be identified and explained. Thus far, we performed numerous MD simulations for atomistic and molecular solids and interpreted the results with the SS-SSM.[7,9–12] In this paper, we demonstrate how the SS-SSM formalism is used to explain the influence of sample material properties on depth profiling quality. The analysis is based on MD results of repetitively bombarded coinage metal samples by a keV C_{60} cluster beam.

Model and previous conclusions

The SS-SSM was described previously in detail.[7] Briefly, the sample is divided into horizontal layers as is applicable to modeling of depth profiling. The material occupation of the layers is given by filling factors. The model constitutes a set of differential equations, which describe how the filling factors change as a function of the amount of eroded material. Each equation contains three terms: a sputtering term describing the loss of material for sputter removal and two displacement terms describing the loss or gain of material for beam-induced material displacements between layers. The model parameters, the sputtering and displacement quantities employed in the equations, are determined from repetitive bombardment MD simulations. The parameters are calculated relative to the average surface level as averages over the impacts within the steady-state range of fluence. The steady-state range of fluence is defined as corresponding to saturated, constant RMS roughness of the sample surface. The sputtering parameters denote the average numbers of atoms sputtered from system layers per impact. Analogously, the displacement parameters denote the average numbers of atoms displaced between system layers per impact. Interchangeably, we use the term 'interlayer mixing' for this type of material displacement in the sample. The model parameters

* Correspondence to: Robert J. Paruch, Department of Chemistry, Penn State University, 104 Chemistry Building, University Park, PA 16802, USA. E-mail: rjp25@psu.edu

a Department of Chemistry, Penn State University, 104 Chemistry Building, University Park, PA, 16802, USA

b Smoluchowski Institute of Physics, Jagiellonian University, ul. Reymonta 4, 30-059 Krakow, Poland

 Copyright © 2014 John Wiley & Sons, Ltd.

establish a microscopic description of sputtering and primary beam-induced displacement phenomena in the system. Usually, we present them in a graphical form of the sputtering and displacement distributions, which is convenient for analyses and making comparisons between systems.[7] Naturally, the sum of all sputtering parameters yields the total sputtering yield. As a new concept suggested by the SS-SSM, we defined the total displacement yield as the sum of all the displacement parameters.[9] The total displacement yield describes numerically the extent of interlayer mixing in the system, that is, the material displacement occurring between horizontal system layers as is appropriate for depth profiling. In contrast to the total sputtering yield, which is independent on the chosen layer thickness, the total displacement yield shows such a dependence and as such is not a well-defined characteristic of the system. It shows utility, however, as a convenient single quantity useful for making comparisons between systems of the same or approximately the same layer thicknesses.

During previous studies, we were interested in how primary beam type and its conditions influence the depth resolution of depth profiling. As a measure of depth profiling quality, we chose one of the depth profile characteristics, namely the full width at half maximum (FWHM).[13] Commonly utilized theoretical models for depth profiling define three contributors to the depth resolution: the information depth, surface roughness, and primary beam mixing described by mixing zone depth.[14,15] The final shape of the depth profile, including its width denoted by FWHM, is a result of an interplay between the three contributors. The three contributors, on the other hand, depend on the conditions under which the depth profiling experiment is performed. In our approach, we tried to use the quantities typical for the SS-SSM to explain how the depth profiling conditions affect its quality. Therefore, we used the total sputtering yield instead of the information depth and the total displacement yield instead of the mixing zone depth. The RMS roughness contributor remains the same as used in both the theoretical models mentioned earlier and the SS-SSM.

We employed this approach to analyze the 'divide and conquer' MD results of Au_3 and C_{60} bombardment of Ag(111) sample.[5] The beam conditions were chosen from ranges of experimental interest, namely beam kinetic energy of 5–20 keV and impact angle of 0–70°. The simulation results were analyzed with the SS-SSM to predict the depth profiles of δ-layers and calculate their FWHMs. We found that, generally, the FWHM correlates with the RMS roughness of the sample. The better depth resolution follows on the beam conditions that result in lower RMS roughness.[9] During further investigation, we found that there is a correlation between the total displacement yield and the RMS roughness of the sample.[9] This observation made us consider the role the displacements play in depth profiling in more detail and finally led us to the conclusion that there is a complementary condition. This condition translated as follows: the best depth profiles occur, when the beam conditions result in large value of the total sputtering yield relative to the value of the total displacement yield. In other words, the ratio of the total sputtering yield to the total displacement yield needs to be maximized.[9]

Description of calculations

We were interested in testing the concepts that resulted from previous applications of the SS-SSM on samples showing various material properties, such as binding energy, mass of constituent atoms, and density. To accomplish this, we used the SS-SSM to interpret the results of MD simulations, where coinage metal samples were repetitively bombarded by a C_{60} beam. The set of samples included Ag, Al, Au, Cu, Ni, Pd, and Pt. For chosen metals, the sublimation energy varies from 2.95 eV for Ag to 5.77 eV for Pt, the mass of constituent atoms from 26.9 amu for Al to 197.0 amu for Au, and the density from 58.6 atom/nm^3 for Ag to 91.4 atom/mn^3 for Ni. The values of sublimation energy were calculated from the molecular dynamics/Monte Carlo corrected effective medium (MD/MC-CEM) interaction potential for metals[16] employed in calculations. The samples measured approximately $53 \times 53 \times 27$ nm, giving the surface area of 2800 nm^2. Approximately 235 impacts were simulated, according to the 'divide and conquer' scheme, for every sample, and the last hundreds of them were used for analysis. This number of impacts was equivalent to the beam fluence of 8.4×10^{12}/cm^2. The calculated number of impact was adequate to observe distinctive trends in RMS roughness and sputtering yield dependences on fluence. In order to calculate the sputtering and displacement parameters of the SS-SSM, the samples were divided into horizontal layers of monoatomic thicknesses. Consequently, for the performed calculations, the δ-layer width was equal to that of a monoatomic layer. Depending on the metal sample and crystal face, it ranged from 0.2025 nm for Al(100) to 0.2361 nm for Ag(111). The δ-layer was located in the sample at the depth of 14 nm. The choice of the δ-layer location in the sample is arbitrary, because the SS-SSM produces steady-state depth profiles. As the SS-SSM model is monocomponent, the δ-layer consisted of the same element as the sample.[7] We also performed a number of simulation with an artificial Morse Ag solid as a help to understand the trends observed in the coinage metal results. In this case, we replaced, normally used in MD calculations, the MD/MC-CEM potential for metals[16] by the Morse potential with parameters that maintain the face centered cubic (FCC) structure of the Ag crystal.[17,18] This allowed us to easily vary the binding energy of the Ag crystal by changing the value of the D parameter (the depth of the well) of the Morse potential. Because this procedure maintains the FCC structure of the Ag crystal, the density of the artificial Ag Morse crystal was equal to the one of the proper Ag crystal.

Results and discussion

Binding energy effect

First, we performed repetitive MD simulations with coinage metal samples, where (111) crystal faces were bombarded by a 20-keV C_{60} beam at 45° incident angle. Coinage metal results turned out to be very similar. The RMS roughness values remained within a factor of two of each other, ranging from 0.84 nm for Pd to 1.72 nm for Ag. The sputtering yields remained within a factor of three of each other, ranging from 158 atoms/impact for Pd to 488 atoms/impact for Ag. The most noticeable correlation of the quantities that influence the depth profile considered here, such as the sputtering yield, displacement yield, and RMS roughness, was with the binding energy of the sample. Consequently, the depth resolution of depth profiling turned out to be mostly affected by the sample binding energy, with bigger binding energies giving better depth profiles. This dependence is shown in Fig. 1, where the sample binding energy is represented by the sublimation energy.

Mass effect

To distinguish between the influence of sample binding energy and the mass of constituent atoms on depth profiling quality,

 Copyright © 2014 John Wiley & Sons, Ltd.

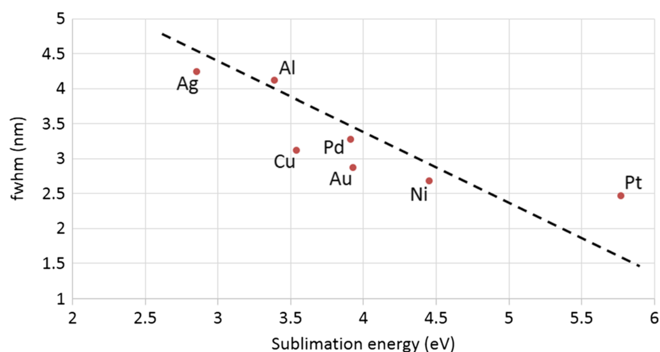

Figure 1. Full width at half maximum of the depth profile dependence on sample sublimation energy for coinage metal samples. The black dashed line is given to guide an eye.

we performed repetitive MD simulations with the artificial Morse Ag crystal bombarded by a 20-keV C_{60} beam at 0° incidence angle. For some of these simulations, we formally changed the mass of Ag atoms in the sample. The mass took values from 58.7 amu (the mass of Ni) to 197.0 amu (the mass of Au). The Morse potential results confirmed the binding energy effect and showed almost no mass effect. As shown in Fig. 2, there is an overall dependence of FWHM on the binding energy of the sample, which is analogous to the dependence shown in Fig. 1 for coinage metals. The FWHM dependence on the mass of constituent atoms is weak. The FWHM values for given binding energies, represented in Fig. 2 by the sublimation energies, vary no more than 9% relative to their average values. Moreover, the data points scatter without order as a function of atomic mass for the given sublimation energies, indicating that, in this case, the depth profiling quality dependence on the mass may be not present at all.

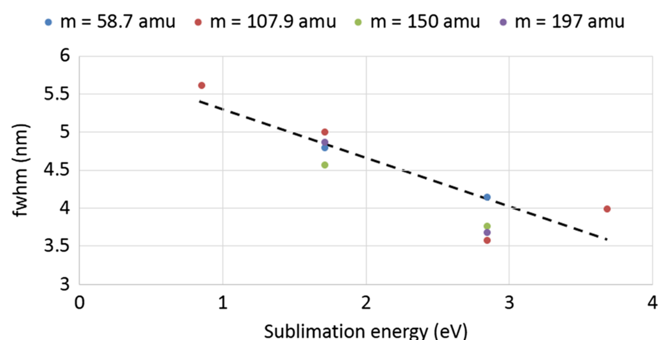

Figure 2. Full width at half maximum of the depth profile dependence on sample sublimation energy and mass of constituent atoms for artificial Morse Ag(111) sample. The black dashed line is given to guide an eye.

The variation of the calculated values and statistics could partly explain the observation. It is daunting, however, to think about calculating the accuracy of the FWHM values, because of the huge computational effort.

Insight from the SS-SSM

The quantities that influence the depth profile calculated for selected coinage MD simulations are presented in Table 1. Al, Ag, and Au have similar lattice constants, 4.05, 4.09, and 4.08 nm, respectively; thus, the atomic density is similar. The mass of constituent atoms varies from 26.9 amu for Al to 197.9 amu for Au, but the effect of mass is weak as the Morse results showed. Consequently, we assumed that for the three metal samples, only the sample binding energy varies significantly among all the factors for depth profiling considered here. The Au sample has the biggest binding energy represented by sublimation energy of 3.93 eV. As expected, based on the overall dependence of FWHM on sample binding energy observed for the whole set of coinage metal samples, shown in Fig. 1, the Au sample gives the best depth profile with the smallest value of FWHM equal to 2.87 nm. The conditions for depth profiling formulated from the SS-SSM studies are fulfilled; namely, for the Au sample, the RMS roughness is the smallest, and the sputtering yield/displacement yield ratio takes the biggest value.

To test the SS-SSM concepts, we also performed MD simulations of 20 keV C_{60} repetitive bombardment of Al samples with conditions as follows: (1) the (100) crystal face irradiated at 45° incident angle at 0° azimuth, (2) the (100) crystal face at 45° incident angle at 45° azimuth, and (3) the (111) crystal face at 45° incident angle at 0° azimuth. The azimuths were chosen relative to the directions in the crystal faces, as explained in Fig. 3a and b, to obtain specific primary beam–sample surface alignments.

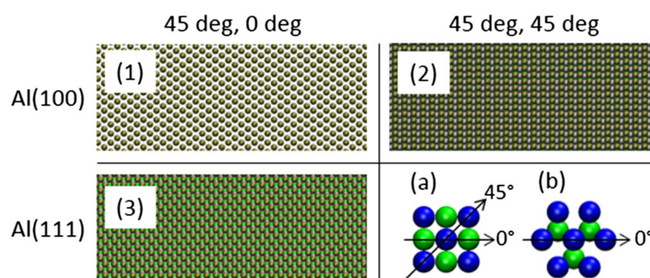

Figure 3. Al sample surfaces (1)–(3) as seen by the primary beam for given crystal faces, and polar and azimuthal angles of incidence. The chosen azimuths relative to the directions in the (a) (100) and (b) (111) crystal faces. Blue and green circles depict the atoms of the first and second atomic layer, respectively.

Table 1. Calculated values of the quantities that influence the depth profile for 20 keV C_{60} bombardment of Al(111), Ag(111), and Au(111) samples

Sample	Sublimation energy (eV)	RMS roughness (nm)	Sputtering yield/displacement yield ratio	FWHM (nm)
Al(111)	3.39	1.54	0.039	4.12
Ag(111)	2.85	1.72	0.059	4.24
Au(111)	3.93	1.19	0.070	2.87

RMS, root mean square; FWHM, full width at half maximum.

Copyright © 2014 John Wiley & Sons, Ltd.

Table 2. Calculated values of the quantities that influence the depth profile for 20 keV C_{60} bombardment of Al samples. The crystal faces, and polar and azimuthal angles of incidence corresponding to cases (1)–(3) are given in Fig 3

Case	RMS roughness (nm)	Sputtering yield/ displacement yield ratio	FWHM (nm)
(1)	1.34	0.024	4.34
(2)	1.55	0.040	3.71
(3)	1.54	0.039	4.12

RMS, root mean square; FWHM, full width at half maximum.

Because sample binding energy and atomic density are the same for the three cases, we assumed that only the beam–surface alignment is a significant factor for depth profiling that varies here. Shown in Fig. 3 are the sample surfaces for the three cases as seen by the primary beam. Only in case (1), there are visible open channels injecting the sample that affect the surface opacity. The average beam penetration depth is 4.5, 3.0, and 2.5 nm for the three cases, respectively. The calculated quantities that influence the depth profile are presented in Table 2. The deepest penetration depth for case (1) result in the worst depth profile with the FWHM equal to 4.34 nm. The sputtering yield/displacement yield ratio takes the smallest value as expected for bad depth profiling conditions in case (1). Of note is that the RMS roughness value is the smallest in case (1). This condition is normally favorable for depth profiling quality; however, the contribution of the low value of the sputtering yield/displacement yield ratio to the depth profile is dominant in this case and overwhelms the effect of the RMS roughness.

As shown in Table 1, the two samples, Al and Ag, that differ in binding energies, RMS roughness values, and the sputtering yield/displacement yield ratios result in depth profiles of comparable FWHM values. Similarly, shown in Table 2 are the cases (2) and (3) that give depth profiles of different FWHM, although their values of RMS roughness and the sputtering yield/displacement yield ratios are comparable. The concept that the best depth profiles occur for a large sputtering yield/displacement yield ratio arose from simulations on one sample, Ag.[9] In addition, a similar change in the sputtering yield/displacement yield ratio can be caused by a variation of either the nominator (the sputtering yield) or the denominator (the displacement yield), both of which could influence the depth profile in a different way. The non-perfect alignment of the FWHM values shown in Tables 1 and 2 with this simple concept is, therefore, possible.

Conclusion

The SS-SSM partnered with MD simulations of repetitive bombardment of solids provides a framework for a quantitative description of the processes that influence depth profiles. Consequently, it is possible to explain how the factors for depth profiling, such as material properties of the sample and primary beam conditions, influence the depth profiling quality. Demonstrated in this paper was this method used to interpret the results of MD simulations of keV C_{60} bombardment of coinage metal samples. The results showed that the most noticeable dependence of depth profiling resolution is on the binding energy of the sample, with bigger binding energies giving better depth profiles. The effect of mass of sample constituent atoms is weak. The depth profiling quality is also affected by the surface opacity; namely, the deeper primary beam penetration depth results in worse depth profiles.

Acknowledgements

The authors gratefully acknowledge the financial support from Polish National Science Center, Program Nos. 2013/09/B/ST4/00094 and PB1839/B/H03/2011/40. We appreciate the support of Penn State Research Computing and Cyberinfrastructure group in performing these simulations.

References

[1] N. Winograd, *Anal. Chem.* **2005**, *77*, 142A.
[2] N. Winograd, B. J. Garrison, *Annu. Rev. Phys. Chem.* **2010**, *61*, 305.
[3] B. J. Garrison, Z. Postawa, *Mass Spectrom. Rev.* **2008**, *27*, 289.
[4] M. F. Russo Jr, Z. Postawa, B. J. Garrison, *J. Phys. Chem. C* **2009**, *113*, 3270.
[5] R. Paruch, L. Rzeznik, M. F. Russo, B. J. Garrison, Z. Postawa, *J. Phys. Chem. C* **2010**, *114*, 5532.
[6] L. Rzeznik, R. Paruch, B. J. Garrison, Z. Postawa, *Nucl. Instrum. Meth. B* **2011**, *269*, 1586.
[7] R. J. Paruch, Z. Postawa, A. Wucher, B. J. Garrison, *J. Phys. Chem. C* **2012**, *116*, 1042.
[8] K. D. Krantzman, A. Wucher, *J. Phys. Chem. C* **2010**, *114*, 5480.
[9] R. J. Paruch, B. J. Garrison, Z. Postawa, *Anal. Chem.* **2012**, *84*, 3010.
[10] B. J. Garrison, R. J. Paruch, Z. Postawa, *Nucl. Instrum. Meth. B* **2013**, *303*, 196.
[11] R. J. Paruch, B. J. Garrison, Z. Postawa, *Surf. Interface Anal.* **2013**, *45*, 154.
[12] R. J. Paruch, B. J. Garrison, Z. Postawa, *Anal. Chem.* **2013**, *85*, 11628.
[13] S. Hofmann, *Surf. Interface Anal.* **2000**, *30*, 228.
[14] S. Hofmann, *Surf. Interface Anal.* **1994**, *21*, 673.
[15] M. G. Dowsett, G. Rowlands, P. N. Allen, R. D. Barlow, *Surf. Interface Anal.* **1994**, *21*, 310.
[16] C. L. Kelchner, D. M. Halstead, L. S. Perkins, N. M. Wallace, A. E. DePristo, *Surf. Sci.* **1994**, *310*, 425.
[17] L. A. Girifalco, V. G. Weizer, *Phys. Rev.* **1959**, *114*, 687.
[18] L. A. Girifalco, V. G. Weizer, in Technical Report R-5, National Aeronautics and Space Administration, **1959**.

Copyright © 2014 John Wiley & Sons, Ltd.